Thin Solid Films 657 (2018) 88–94

Contents lists available at ScienceDirect

Thin Solid Films

journal homepage: www.elsevier.com/locate/tsf

Electrospinning superhydrophobic nanofibrous poly(vinylidene fluoride)/stearic acid coatings with excellent corrosion resistance

Mengke Cui[a], Changcheng Xu[a], Yongqian Shen[b,*], Haifeng Tian[a], Hua Feng[a], Jian Li[a,*]

[a] College of Chemistry and Chemical Engineering, Northwest Normal University, Lanzhou 730070, PR China
[b] State Key Laboratory of Advanced Processing and Recycling of Non-ferrous Metals, Key Laboratory of Nonferrous Metal alloys and Processing, Ministry of Education, School of Materials Science & Engineering, Lanzhou University of Technology, Lanzhou 730050, China

ARTICLE INFO

Keywords:
Superhydrophobicity
Electrospun
Polyvinylidenefluoride
Coating
Anti-corrosion

ABSTRACT

Due to the unique micro/nanoscale rough surface structures and water-repellency, the superhydrophobic surfaces hold great potential of anti-corrosive protection. This study reported a facile and controllable electrospinning technology to fabricate polyvinylidenefluoride (PVDF)/stearic acid (SA) nanofibers onto metal substrates for long-time anti-corrosive protection. Moreover, the anti-corrosion performances of the superhydrophobic nanofibers coated metal substrates were characterized by the Tafel polarization curve and electrochemical impedance spectroscopy (EIS). In addition, the electrochemical corrosion test results demonstrated the superhydrophobic PVDF/SA nanofibrous coatings possessed superior anti-corrosion performances for long-term metal substrates preservation, even after being immersed in a 3.5 wt% NaCl aqueous solutions up to 30 days. Therefore, we deeply believe the superhydrophobic PVDF/SA nanofibrous coatings could present a superior application prospect in anti-corrosive protection.

1. Introduction

Since 1997, when Barthlott and Neinhuis firstly revealed the superhydrophobic phenomenon on the natural lotus leaf surface [1,2], and this special phenomenon was subsequently discovered on various surfaces of plants' leaves [3], petals of several flowers [4] and body cortexes of diverse insects [5] with their water contact angles (WCAs) larger than 150°. As well known, a surface with WCAs greater than 150° and sliding angles of less than 10° could be supported to be a superhydrophobic surface [6–8]. In recent years, biomimetic superhydrophobic surfaces have been widely fabricated and exhibited remarkable significance application value in many fields [9], such as self-cleaning [10], anti-fogging [11], anti-corrosion [12], anti-icing [13], oil/water separation [14], selective liquid transportation [15] and so forth. Generally, three strategies were existed for fabricating a superhydrophobic surface [16,17]. One is simply enhance the micro-/nano-scale roughness, the other is only modifying with the low-surface-energy compounds, the third is one or more steps combination of both afore-procedures [18]. Even though the former two strategies could achieve the transition from hydrophobicity to superhydrophobicity on the basis of Wenzel and Cassie models [19,20], they are nonstable. The strategy of effectively co-operation of micro-/nano-scale rough structure and low-surface-energy compounds on a surface, which can contribute to a better stable superhydrophobic surface with excellent anti-corrosion property. In depth, the suitable rough structure of a superhydrophobic surface could trap a small amount of air to prevent water, moisture and corrosive solutions from reaching the base, and the low-surface-energy compounds can provide a lower surface energy, which was essential for generating a stable superhydrophobic surface [21–23]. To the best of our knowledge, traditional fabrication methods of superhydrophobic surfaces are always involving two steps: firstly creating rough structure and then modified with low-surface-energy materials, which are very cumbersome [24,25]. Thus, we envisage that if the two steps that traditional superhydrophobic surface fabrication processes involved could accomplish in just a single procedure, and thus the complexity of developing procedures could be omitted. Herein, the stable superhydrophobic surfaces are fabricated by using the simple one-step process, electrospinning technology to spin superhydrophobic polymer nanofibers onto many metal substrates.

Furthermore, long-time anti-corrosive property was very important for real application of superhydrophobic surfaces as a result of the corrosive environments that metal substrates faced is becoming increasingly serious. Besides, corrosion always causes huge economic loss every year in both developed and under developing countries. Corrosion of metal substrates is one of the major problems in contemporary society and industrial sector. Generally, the formations of

* Corresponding authors.
E-mail addresses: syqch@163.com (Y. Shen), jianli83@126.com (J. Li).

https://doi.org/10.1016/j.tsf.2018.05.008
Received 31 October 2017; Received in revised form 4 May 2018; Accepted 4 May 2018
Available online 05 May 2018
0040-6090/

metal oxide film such Cr_2O_3 film on the surface of metal substrates is used to control its corrosion in aggressive medium. Nowadays, chromate treatment is still widely used to promote the formation of the film in order to protect stainless steel mesh [26]. However, Cr (VI) is a carcinogenic agent [27]. In addition, such treatment would pose an unrepairable damage to substrates. As a consequence, it is imperative to conduct a superwetting material to replace the use of toxic chromates with green anti-corrosion coatings.

As we all known, polyvinylidenefluoride (PVDF) is commonly used polymer materials because of its excellent antioxidation and anti-corrosion property, favorable thermal stability and good mechanical behaviour [28,29]. In addition, the PVDF polymers are intrinsically hydrophobicity (WCAs of 130 ± 1°) but they are not superhydrophobicity, which brings many difficulties for long-time anti-corrosive protection. To overcome this, stearic acid (SA) was mixed into the PVDF polymer for obtaining a PVDF/SA polymer with superhydrophobic property. Herein, the simple, low-cost electrospinning technique was used to construct a superhydrophobic surface onto many metal substrates. Moreover, the obtained PVDF/SA nanofibers coated substrates demonstrated excellent superhydrophobicity with WCAs of 155 ± 2°. Furthermore, the long-time corrosion behaviors of the pure PVDF, superhydrophobic PVDF/SA nanofibers coated Al sheets and bare Al sheet were respectively investigated by the Tafel polarization curve and electrochemical impedance spectroscopy (EIS). The results indicated that superhydrophobic PVDF/SA nanofibrous coatings exhibited excellent long-time corrosion resistance than that of pure PVDF nanofibrous coatings. To sum up, the superhydrophobic PVDF/SA nanofibrous coatings presented a superior application value in long-time anti-corrosive protection.

2. Experimental

2.1. Materials

Polyvinylidenefluoride (PVDF) was purchased from Xiya Chemical Industry Co. Ltd., Shandong, China. *N*,*N*-dimethylformamide (DMF) was purchased from Guangdong Guanghua Technology Co., Ltd., Guangdong, China. Stearic acid (SA) was purchased from Shanghai Shan Pu Chemical Co., Ltd., Shanghai, China.

2.2. Preparation of PVDF/SA nanofibrous membranes

Firstly, the SA (2 g) was dissolved into 10 mL of acetone/DMF (4/1, mL/mL) to obtain SA solution. Subsequently, 8 g of PVDF powder was added into the SA solution. Finally, the obtained PVDF/SA solution was magnetically stirred for 10 h at room temperature (25 °C) to produce the homogeneous solution. Herein, acetone and DMF acted as solvents in the processes of electrospinning solution generation. An electrospinning setup was used to spin nanofibers onto many metal substrates (Such as Al sheet, mesh) at room temperature (25 °C) with a positive voltage of 16 kV applied on the needle and a negative voltage of 2 kV applied on the collecting substrate. The distance between the spinneret and the collector substrate was 15 cm. The rate of solution flow was set at 0.8 mL/h through a syringe pump, and the ambient relative humidity was around 40%. After being proceeded for 30 min, the as-prepared nanofibrous membranes were dried at 80 °C for 2 h to remove the residual solvent. Pure PVDF nanofibrous membranes were also prepared as a reference to compare with PVDF/SA membranes.

2.3. Electrochemical corrosion studies

Electrochemical corrosion measurements were carried out in a 3.5 wt% NaCl solution using a computer-controlled CHI600E electrochemical workstation. A conventional three-electrode system was utilized with a saturated Ag/AgCl as the reference electrode, a platinum plate as the counter electrode and the samples (bare Al sheet, PVDF nanofibers coated Al sheet and PVDF/SA nanofibers coated Al sheet that after immersion in 3.5 wt% NaCl solutions for different time) with an exposed area of 1 cm^2 as the working electrode. At first, the superhydrophobic nanofibers coated sample was immersed in a 3.5 wt% NaCl corrosive solution to establish the open circuit potential (E_{ocp}). Tafel polarization curves were obtained at a potential sweep rate of 1 mV s^{-1}, and the corrosion data were obtained through superimposing a straight line along the linear portion of the cathodic and anodic curves. The electrochemical impedance spectroscopy (EIS) measurements were conducted at E_{ocp} in the frequency ranged from 10 mHz to 100 kHz with two cycles at each frequency using an ac perturbation of 5 mV. Impedance data were analyzed by using ZSimpWin software.

2.4. Instrumentations and characterization

The electrospinning setup was composed of high voltage DC power (DW-P503-1ACDF, Tianjin, China) and electrospinning machine (JDF05, Changsha, China). Morphological analysis of the nanofibrous membranes was performed using a field-emission scanning electron microscope (FE-SEM, Zeiss). Static water contact angle (WCA) values were obtained using an SL200KB apparatus at ambient temperature with 5 μL of distilled water on the surface of nanofibrous membranes. Fourier transform infrared (FT-IR) spectroscopy was performed with a Bio-Rad FTS-165 instrument. Electrochemical measurements were carried out by using a computer-controlled CHI660E electrochemical workstation.

3. Results and discussion

Fig. 1 demonstrated the fabrication process of the superhydrophobic PVDF/SA nanofibrous membrane with its applications in anti-corrosion. The electrospinning solution was prepared by simply mixing PVDF and SA into DMF/acetone solutions, and then magnetically stirred for 10 h. The details of fabrication process of PVDF/SA nanofibrous membranes are displayed in the Experimental Section. The fabrication process of the PVDF/SA nanofibrous membranes is extremely facile, low-

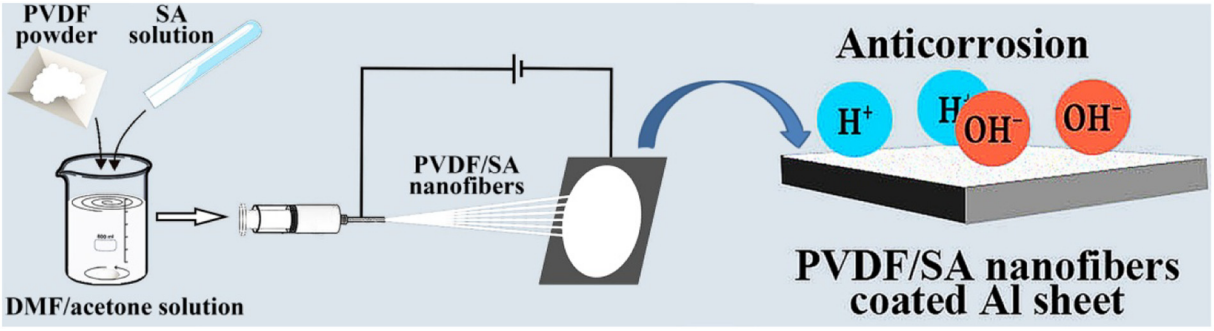

Fig. 1. Illustration of fabrication process of the PVDF/SA nanofibrous coatings via electrospinning technology, and their applications of anti-corrosive protection.

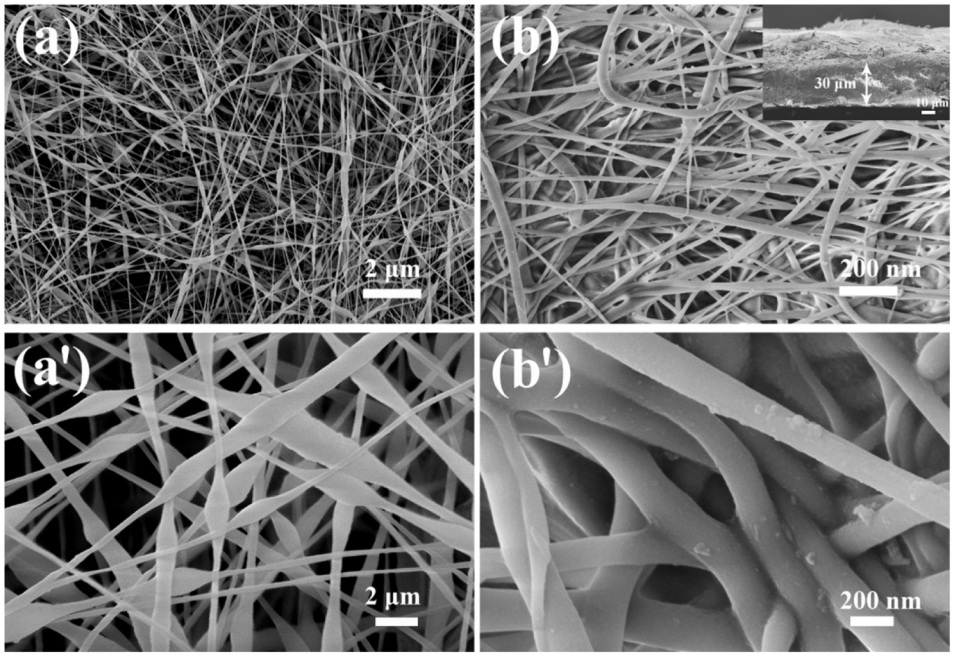

Fig. 2. (a, a′) FE-SEM images of pure PVDF nanofibrous coating. (b, b′) FE-SEM images of PVDF nanofibrous coating.

cost and easily scaled up, which possessed excellent application value in anti-corrosive protection.

The morphologies of the as-prepared PVDF/SA and pure PVDF nanofibrous membranes were studied by FE-SEM. Without SA mixing, the pure PVDF nanofibers exhibited spider web-like structure with an average diameter around 50 nm, as shown in Fig. 2a. Moreover, it also can be seen that the knot-like structures are regularly distributed in pure PVDF nanofibers with a smooth surface (Fig. 2a′). The well distributed spindle-knot and joint structures in the nanofibers led to a rough surface of the pure PVDF nanofibrous membranes. After addition of SA, the diameter of the PVDF/SA nanofibers increased and spindle-knot and joint structures disappeared (Fig. 2b). Here, it should be mentioned that the thickness of as-prepared PVDF/SA nanofibrous membranes is about 30 μm (Fig. 2b′). Besides, a lot of nano-scale debris appeared on the surface of PVDF/SA nanofibers, indicating SA was successfully blended into the PVDF nanofibers. Therefore, the nano/micro-scale debris not only greatly enhanced the roughness of nanofibrous surfaces, but also endowed the surface of nanofibers a lower surface energy.

The wettability property of the pure PVDF nanofibrous coating blended into SA before and after was evaluated by WCA measurements. As shown in Fig. 3a, the WCA of pure PVDF nanofibrous coating is approximately 130 ± 1°. While, the WCA of PVDF/SA nanofibrous coating is up to 155 ± 2° (Fig. 3a), demonstrating excellent superhydrophobicity. Moreover, the increase of WCAs is possibly contributed to the synergetic effect of the lower free surface energy of SA and the enhanced surface roughness [30–32]. Besides, the adhesion capability of PVDF/SA nanofibrous coating was evaluated by water sliding angle measurement. As shown in Fig. 3c, the sliding angle of PVDF/SA nanofibrous coating was measured to be approximately 5 ± 1°, indicating lower adhesion force. Furthermore, the PVDF/SA nanofibrous coating also exhibited excellent superhydrophobic stability. As shown in Fig. 3d, the WCA of PVDF/SA nanofibrous coating after immersing in 3.5 wt% NaCl for 30 days and then washed by ethanol was approximately 151 ± 1°, illustrating better anti-corrosive stability.

Furthermore, the anti-corrosive property of as-prepared PVDF/SA nanofibrous coatings was sufficiently investigated for evaluating their possibility of practical applications in corrosive mediums [33–36]. Therein, the Tafel polarization curve is the most efficient method to detect the anti-corrosion performances of surperhydrophobic coatings for metal surface protection. In a typical Tafel polarization curve, the excellent corrosion resistance always possesses a lower corrosion rate (C_R), which corresponds to a higher corrosion potential (E_{corr}) or a lower corrosion current density (I_{corr}) [37–40]. The corrosion resistance of the superhydrophobic PVDF/SA nanofibrous coatings was tested in a 3.5 wt% NaCl aqueous solution by the way of electrochemistry. Fig. 4 displayed the Tafel polarization curves of bare Al sheet, pure PVDF and PVDF/SA nanofibers coated Al sheet after immersion in 3.5 wt% NaCl aqueous solutions for different times at room temperature. The Tafel regions can be easily identified from the anodic and cathodic curves and corresponding corrosion data obtained by using the Tafel extrapolation method are given in Table 1. The C_R values of the bare Al sheet, pure PVDF and PVDF/SA nanofibers coated samples were calculated by the following equation [41]:

$$\mathbf{C_R = 3270} \times \frac{\boldsymbol{I_{corr} M}}{\boldsymbol{VD}} \tag{1}$$

where $\mathbf{3270} = 0.01 \times [1\text{ year (in s)}/96{,}497.8]$ and 96,497.8 = 1 F in Coulombs. $\boldsymbol{M}$ is the atomic mass of Al, $\boldsymbol{I_{corr}}$ is determined by an intersection of the linear portions of the anodic and cathodic sections of the Tafel curves, $\boldsymbol{V}$ is the valence (the number of electrons that are lost during the oxidation reaction), and $\boldsymbol{D}$ is the density of Al sheet [42,43].

The corresponding corrosion data of bare Al sheet, pure PVDF and PVDF/SA nanofibers coated samples were presented in Table 1. It can be easily seen that the E_{corr} of superhydrophobic PVDF/SA nanofibers coated samples immersed in 3.5 wt% NaCl solution for 6 h is still larger than that of pure PVDF nanofibers coated samples and bare Al sheets. Moreover, the I_{corr} and C_R of the PVDF/SA nanofibers coated samples immersed in 3.5 wt% NaCl solution for 6 h are nearly 400 times smaller than that of pure PVDF nanofibers coated samples. More importantly, the I_{corr} and C_R of the PVDF/SA nanofibers coated samples after immersion in 3.5 wt% NaCl solution for 30 days are still 100 times smaller than that of pure PVDF nanofibers coated samples and kept almost as the same as that of the PVDF/SA nanofibers coated samples after immersion for 6 h, indicating excellent long-time anti-corrosive performances. From what has been discussed above, we can conclude that the as-fabricated PVDF/SA nanofibrous coatings exhibited outstanding anti-corrosive property for long-time metal substrates preservation than that of pure PVDF nanofibrous coatings.

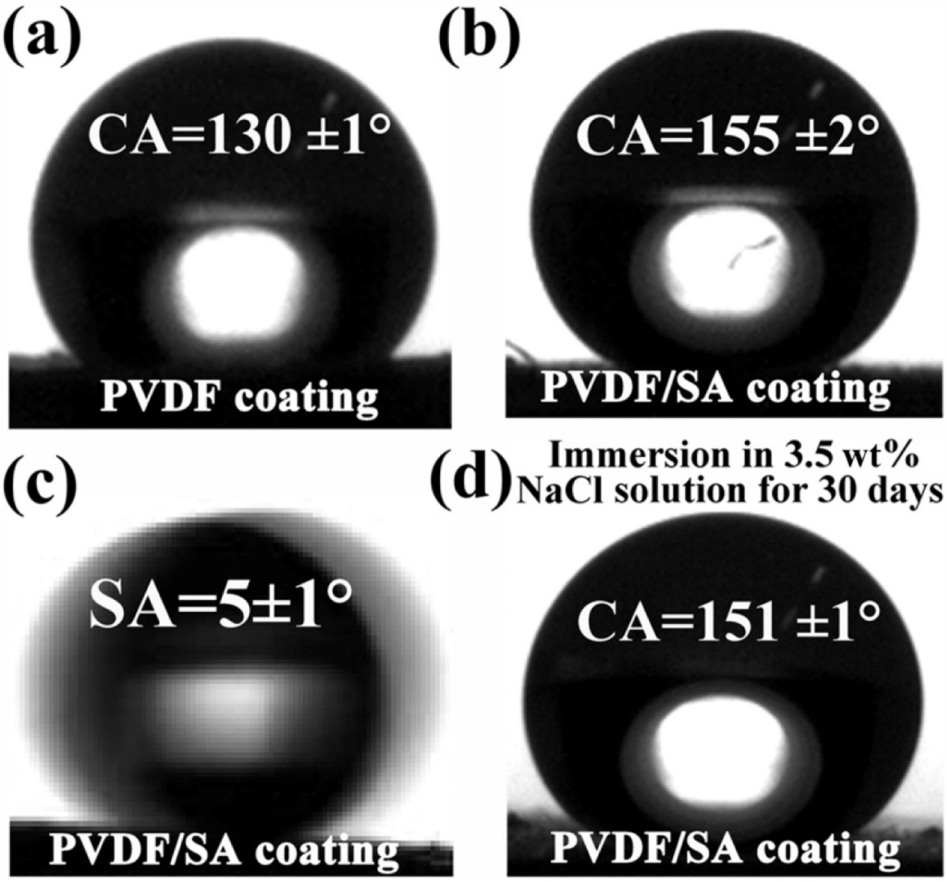

Fig. 3. The WCA of (a) pure PVDF nanofibrous coating and (b) PVDF/SA nanofibrous coating. (c) The sliding angle of PVDF/SA nanofibrous coating. (d) The WCA of PVDF/SA nanofibrous coating that was immersed in 3.5 wt% NaCl solutions for 30 days.

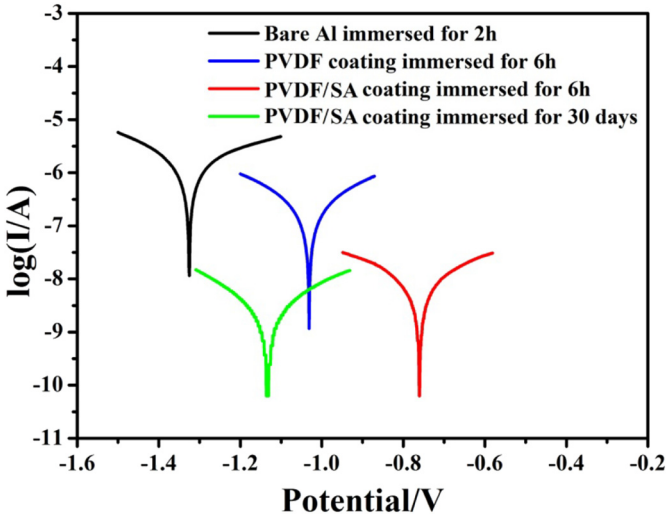

Fig. 4. Tafel polarization curves of a bare Al sheet substrate after immersion in a 3.5 wt% NaCl aqueous solution for 2 h and pure PVDF nanofibers coated Al sheet after immersion in 3.5 wt% NaCl aqueous solutions for 6 h, and PVDF/SA nanofibers coated Al sheet after immersion in 3.5 wt% NaCl aqueous solutions for 6 h and 30 days, respectively.

The electrochemical impedance spectroscopy (EIS) was further used to characterize the corrosion behaviors of bare Al sheet, pure PVDF and PVDF/SA nanofibers coated samples. The EIS measurements were performed under open circuit potential in 3.5 wt% NaCl corrosive solutions with a frequency ranging from 10 mHz to 100 kHz. Fig. 5a depicts the evolution of the impedance spectra of bare Al, pure PVDF and PVDF/SA nanofibers coated samples after immersion in a 3.5 wt% NaCl solutions for different time. It can be seen that the EIS spectra of such samples displayed a large semicircle and a tail, in which the diameter of the large semicircle (also termed as high-frequency capacitive loop) in the impedance plots signifies the polarization resistance of the nanofibrous coatings and a tail (also termed as low-frequency capacitive loop) is influenced by electron diffusion. It also can observe that the loops of the impedance spectra of the PVDF/SA nanofibers coated samples after immersion in 3.5 wt% NaCl solutions for 30 days are larger than that of PVDF/SA, pure PVDF nanofibers coated samples after immersion in 3.5 wt% NaCl solutions for 6 h and bare Al sheet (Fig. 5a). In addition, the loops of the impedance spectra of PVDF/SA nanofibrous coatings enhanced greatly with the increment of their immersion time. Besides, the PVDF/SA nanofibers coated samples after immersion in 3.5 wt% NaCl solutions for 6 h exhibited a higher impedance value than that of the interface for pure PVDF nanofibers coated samples and bare Al sheet. The results of the impedance spectra agree well with the bode plot of impedance modulus |Z| as a function of frequency. As shown in Fig. 5b, we can observe that the impedance modulus |Z| of the PVDF/SA nanofibers coated samples after immersion for 6 h remained high value of approximately $8.711 \times 10^6\ \Omega\,cm^2$ at low frequency, which is about 40 times higher than that of pure PVDF nanofibers coated samples and 500 times higher than that of bare Al sheet. In addition, the impedance modulus |Z| value of the PVDF/SA nanofibrous coating slightly increased at low frequency and decreased greatly at high frequency with the immersion time up to 30 days. Moreover, the impedance modulus |Z| value of PVDF/SA nanofibrous coating after immersion in 3.5 wt% NaCl solutions for 30 days at low frequency maintained about $1.354 \times 10^6\ \Omega\,cm^2$, which is about 20 times higher

Table 1
Corresponding corrosion data of following samples after immersion in 3.5 wt% NaCl solution for different time obtained from a Tafel polarization measurement.

Samples	Bare Al	PVDF-Al	PVDF/SA-Al	PVDF/SA-Al
Corrosion time	2 h	6 h	6 h	30 days
E_{corr} (eV)	−1.325	−1.031	−0.765	−1.133
I_{corr} (A cm^{-2})	1.488×10^{-6}	2.055×10^{-7}	8.095×10^{-9}	8.125×10^{-9}
C_R (mm year^{-1})	0.01622	2.240×10^{-6}	8.824×10^{-8}	8.829×10^{-8}

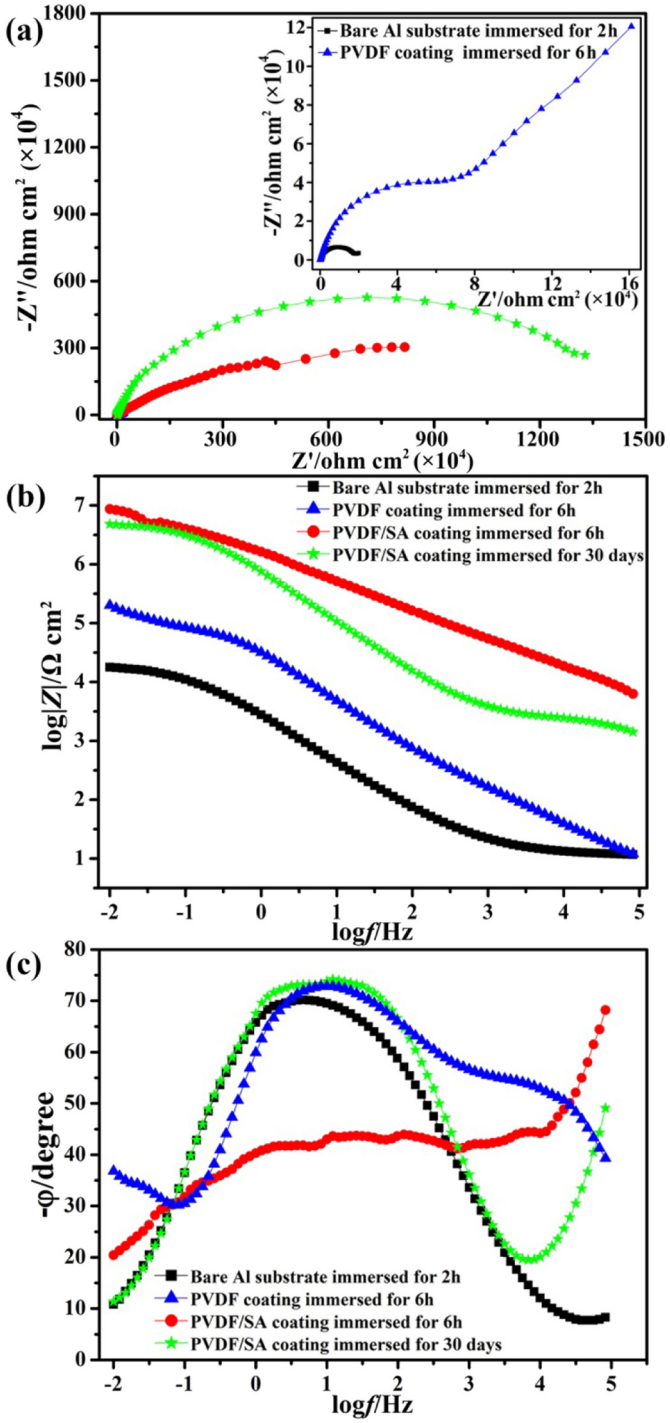

Fig. 5. EIS results of bare, PVDF and PVDF/SA nanofibers coated Al surfaces in 3.5 wt% NaCl solution after different immersion time. (a) Nyquist plots, (b) bode |Z| versus frequency plots, and (c) bode phase angle versus frequency plots.

than the resistance of pure PVDF nanofibrous coatings. As shown in Fig. 5c, the EIS spectra of the PVDF/SA nanofibers coated samples after immersion in a 3.5 wt% NaCl solution for 6 h presented a steady upward trend from low frequency to medium frequency, and a rapid upward trend at high frequency. In addition, the EIS spectra of the bare Al, pure PVDF nanofibers coated samples and PVDF/SA nanofibers coated samples after immersion for 30 days displayed one phase at medium frequency. Moreover, it also can be seen that with the immersion time increasing from 6 h to 30 days, a phase maximum appeared at medium frequency in the EIS spectra of the PVDF/SA nanofibers coated samples. Furthermore, at high frequency, the value of $-\varphi$ of PVDF/SA nanofibers coated samples after immersion in 3.5 wt% NaCl solution for 30 days was still larger than that of pure PVDF nanofibers coated samples immersion for 6 h, indicating excellent anti-corrosive performances for long-term metal substrates protection.

Both Tafel polarization curve and EIS results indicated that the addition of SA could improve the corrosion resistance of the pure PVDF nanofibrous coatings significantly and the PVDF/SA nanofibrous coatings showed excellent anti-corrosive property. The excellent anti-corrosive performances of the superhydrophobic PVDF/SA nanofibrous coatings is contributed to the synergistic effect of the small amount of air trapped in rough porous structures and the superhydrophicity of PVDF/SA nanofibers. Essentially, such synergistic effect is reducing the contact area between corrosive solutions and metal substrates, which can be illustrated by its corrosion resistant mechanism (Fig. 6). Specifically, (1) the Al_2O_3 film has an anti-corrosion performance inherently. (2) The PVDF/SA nanofibrous coatings could generate a physical barrier effect for corrosive solutions. (3) The small amount of air trapped in micro-pores structures provides an extra barrier layer to obstruct corrosive solutions permeation, which plays an important role to prevent corrosive solutions from touching the underlying metals. (4) The well-dispersed superhydrophobic SA could reinforce the anti-corrosion performance of PVDF nanofibrous coatings, owing to it could significantly reduce the contact area between corrosive solutions and underlying metals [44]. Herein, various shapes of the pores in the PVDF/SA nanofibrous coatings were assumed to be cylindrical pores. Thus, the reduction of contact area can be characterized by Yang-Laplace equation:

$$\Delta \boldsymbol{p} = \gamma\left(\frac{1}{\boldsymbol{R}} - \frac{1}{\boldsymbol{R'}}\right) \tag{2}$$

where $\Delta \boldsymbol{p}$ is the pressure difference between the liquid surface and gas surface, γ is the liquid surface tension, $\boldsymbol{R}$ is the radius of the pores and $\boldsymbol{R'}$ is the radius of the curved liquid surface. As presented in Fig. 6, it can be clearly seen that the radius of the curved liquid surface (R_1) of PVDF nanofibrous coatings is larger than that (R_2) of PVDF/SA nanofibrous coatings, which was due to the CA of PVDF/SA nanofibrous coatings is greater than that of PVDF nanofibrous coatings. Based on Eq. (2), we can find that Δp_2 is greater than Δp_1 in Fig. 6, which indicated the PVDF/SA nanofibrous coatings could provide larger capillary force to prevent corrosive solutions intrusion. It is known to all that the pressure value is inversely proportional to the contact area. Therefore, we can conclude that after adding SA, the contact area between corrosive liquids and metal substrate was significantly reduced.

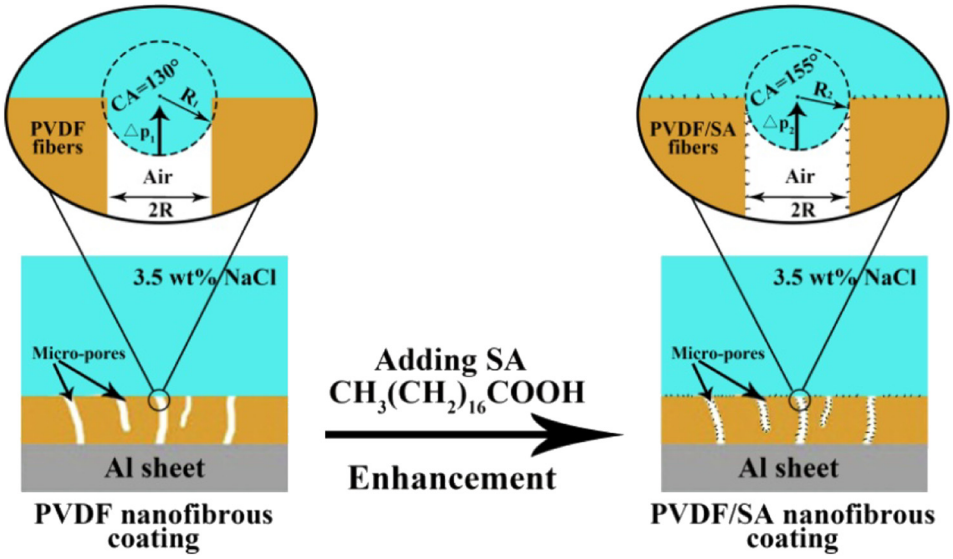

Fig. 6. Schematic representation of the corrosion resistant mechanisms of the superhydrophobic PVDF/SA nanofibrous coatings.

4. Conclusion

In summary, a facile, low-cost electrospinning technique was employed to construct the superhydrophobic PVDF/SA nanofibrous coatings. Moreover, the as-fabricated PVDF/SA nanofibers coated aluminum substrate exhibited larger impedance and lower corrosion current density than does the PVDF nanofibers coated aluminum substrate, even for 30 days of immersion in a 3.5 wt% NaCl corrosive solution, which demonstrated the superhydrophobic PVDF/SA nanofibrous coatings possessed superior anti-corrosion performances for long-term metal substrates preservation. Therefore, the as-prepared superhydrophobic PVDF/SA nanofibrous coatings hold great potential in anti-corrosive protection.

Acknowledgements

This project was funded by the Fok Ying-Tong Education Foundation, China (161044), China Postdoctoral Science Foundation (2017M610031) and the Yong Teacher Research Group Foundation of Northwest Normal University (NWNU-LKQN-16-6).

References

[1] M.A. Shannon, P.W. Bohn, M. Elimelech, J.G. Georgiadis, B.J. Mariñas, A.M. Mayes, Science and technology for water purification in the coming decades, Nature 452 (2008) 301–310.
[2] Z. Chu, Y. Feng, S. Seeger, Oil/water separation with selective superantiwetting/superwetting surface materials, Angew. Chem. Int. Ed. 54 (2015) 2328–2338.
[3] B. Wang, W. Liang, Z. Guo, W. Liu, Biomimetic super-lyophobic and super-lyophilic materials applied for oil/water separation: a new strategy beyond nature, Chem. Soc. Rev. 44 (2015) 336–361.
[4] B.R. Solomon, N. Hyder, K.K. Varanasi, Separating oil–water nanoemulsions using flux-enhanced hierarchical membranes, Sci. Rep. 4 (2014) 5504–5509.
[5] M. Tao, L. Xue, F. Liu, L. Jiang, An intelligent superwetting PVDF membrane showing switchable transport performance for oil/water separation, Adv. Mater. 26 (2014) 2943–2948.
[6] V. Broje, A. Keller, Improved mechanical oil spill recovery using an optimized geometry for the skimmer surface, Environ. Sci. Technol. 40 (2006) 7914–7918.
[7] S. Song, H. Yang, C. Zhou, J. Cheng, Z. Jiang, Z. Lu, J. Miao, Underwater superoleophobic mesh based on $BiVO_4$ nanoparticles with sunlight-driven self-cleaning property for oil/water separation, Chem. Eng. J. 320 (2017) 342–351.
[8] J. Li, D. Li, Y. Yang, J-ping Li, F. Zha, Z. Lei, A prewetting induced underwater superoleophobic or underoil (super) hydrophobic waste potato residue-coated mesh for selective efficient oil/water separation, Green Chem. 18 (2016) 541–549.
[9] C. Su, H. Yang, S. Song, B. Lu, R. Chen, A magnetic superhydrophilic/oleophobic sponge for continuous oil-water separation, Chem. Eng. J. 309 (2017) 366–373.
[10] J. Li, C. Xu, Y. Zhang, R. Wang, F. Zha, H. She, Robust superhydrophobic attapulgite coated polyurethane sponge for efficient immiscible oil/water mixture and emulsion separation, J. Mater. Chem. A 4 (2016) 15546–15553.
[11] L. Feng, Z. Zhang, Z. Mai, Y. Ma, B. Liu, L. Jiang, D. Zhu, A super-hydrophobic and super-oleophilic coating mesh film for the separation of oil and water, Angew. Chem. Int. Ed. 43 (2004) 2012–2014.
[12] Y. Raghupathy, A. Kamboj, M.Y. Rekha, RaoN.P. Narasimha, C. Srivastava, Copper-graphene oxide composite coatings for corrosion protection of mild steel in 3.5% NaCl, Thin Solid Films 636 (2017) 107–115.
[13] D. Zang, C. Wu, R. Zhu, W. Zhang, X. Yu, Y. Zhang, Porous copper surfaces with improved superhydrophobicity under oil and their application in oil separation and capture from water, Chem. Commun. 49 (2013) 8410–8412.
[14] Y. Hu, Y. Zhu, H. Wang, C. Wang, H. Li, X. Zhang, R. Yuan, Y. Zhao, Facile preparation of superhydrophobic metal foam for durable and high efficient continuous oil-water separation, Chem. Eng. J. 322 (2017) 157–166.
[15] J. Li, L. Yan, H. Li, J. Li, F. Zha, Z. Lei, A facile one-step spray-coating process for the fabrication of a superhydrophobic attapulgite coated mesh for use in oil/water separation, RSC Adv. 5 (2015) 53802–53808.
[16] J. Yang, L. Yin, H. Tang, H. Song, X. Gao, K. Liang, C. Li, Polyelectrolyte-fluorosurfactant complex-based meshes with superhydrophilicity and superoleophobicity for oil/water separation, Chem. Eng. J. 268 (2015) 245–250.
[17] S. Li, J. Huang, Z. Chen, G. Chen, Y. Lai, Review on special wettability textiles: theoretical models, fabrication technologies and multifunctional applications, J. Mater. Chem. A 5 (2017) 31–55.
[18] S.V. Gnedenkov, S.L. Sinebryukhov, V.S. Egorkin, I.E. Vyaliy, Wettability and electrochemical properties of the highly hydrophobic coatings on PEO-pretreated aluminum alloy, Surf. Coat. Technol. 307 ((2016) 1241–1248.
[19] J. Li, L. Yan, Y. Zhao, F. Zha, Q. Wang, Z. Lei, One-step fabrication of robust fabrics with both-faced superhydrophobicity for the separation and capture of oil from water, Phys. Chem. Chem. Phys. 17 (2015) 6451–6457.
[20] W. Yang, J. Li, P. Zhou, L. Zhu, H. Tang, Superhydrophobic copper coating: switchable wettability, on-demand oil-water separation, and antifouling, Chem. Eng. J. 327 (2017) 849–854.
[21] W. Zhang, Y. Zhu, X. Liu, D. Wang, J. Li, L. Jiang, J. Jin, Salt-induced fabrication of superhydrophilic and underwater superoleophobic PAA-g-PVDF membranes for effective separation of oil-in-water emulsions, Angew. Chem. Int. Ed. 53 (2014) 856–860.
[22] L. Chen, Y. Si, H. Zhu, T. Jiang, Z. Guo, A study on the fabrication of porous PVDF membranes by in-situ elimination and their applications in separating oil/water mixtures and nano-emulsions, J. Membr. Sci. 520 (2016) 760–768.
[23] X. Yuan, W. Li, Z. Zhu, N. Han, X. Zhang, Thermo-responsive PVDF/PSMA composite membranes with micro/nanoscale hierarchical structures for oil/water emulsion separation, Colloids Surf. A 516 (2017) 305–316.
[24] Y. Li, Z. Zhang, B. Ge, X. Men, Q. Xue, A versatile and efficient approach to separate both surfactant-stabilized water-in-oil and oil-in-water emulsions, Sep. Purif. Technol. 176 (2017) 1–7.
[25] W. Zhang, N. Liu, Y. Cao, Y. Chen, L. Xu, X. Lin, L. Feng, A solvothermal route decorated on different substrates: controllable separation of an oil/water mixture to a stabilized nanoscale emulsion, Adv. Mater. 27 (2015) 7349–7355.
[26] A.I. Munoz, J.G. Anton, J.L. Guinon, V.P. Herranz, Inhibition effect of chromate on the passivation and pitting corrosion of a duplex stainless steel in LiBr solutions using electrochemical techniques, Corros. Sci. 49 (2007) 3200–3225.
[27] M. Ding, X. Shi, Molecular mechanisms of Cr(VI)-induced carcinogenesis, Mol. Cell. Biochem. 234 (2002) 293–300.
[28] F. Liu, N.A. Hashim, Y.T. Liu, M.R.M. Abed, K. Li, Progress in the production and modification of PVDF membranes, J. Membr. Sci. 375 (2011) 1–27.
[29] G.D. Kang, Y.M. Cao, Application and modification of poly(vinylidene fluoride) (PVDF) membranes, J. Membr. Sci. 463 (2014) 145–165.
[30] J. Li, Z. Jing, F. Zha, Y. Yang, Q. Wang, Z. Lei, Facile spray-coating process for the

fabrication of tunable adhesive superhydrophobic surfaces with heterogeneous chemical compositions used for selective transportation of microdroplets with different volumes, ACS Appl. Mater. Interfaces 6 (2014) 8868–8877.
[31] Y. Tian, B. Su, L. Jiang, Interfacial material system exhibiting superwettability, Adv. Mater. 26 (2014) 6872–6897.
[32] S. Wang, K. Liu, X. Yao, L. Jiang, Bioinspired surfaces with superwettability: new insight on theory, design, and applications, Chem. Rev. 115 (2015) 8230–8293.
[33] Q. Liu, D. Chen, Z. Kang, One-step electrodeposition process to fabricate corrosion-resistant superhydrophobic surface on magnesium alloy, ACS Appl. Mater. Interfaces 7 (2015) 1859–1867.
[34] D. Zhang, L. Wang, H. Qian, X. Li, Superhydrophobic surfaces for corrosion protection: a review of recent progresses and future directions, J. Coat. Technol. Res. 13 (2016) 11–29.
[35] L. Zhao, Q. Liu, R. Gao, J. Wang, W. Yang, L. Liu, One-step method for the fabrication of superhydrophobic surface on magnesium alloy and its corrosion protection, antifouling performance, Corros. Sci. 80 (2014) 177–183.
[36] N.S. Manam, W.S.W. Harun, D.N.A. Shri, S.A.C. Ghani, T. Kurniawan, M.H. Ismail, M.H.I. Ibrahim, Study of corrosion in biocompatible metals for implants: a review, J. Alloys Compd. 701 (2017) 698–715.
[37] Y. Qing, C. Yang, N. Yu, Y. Shang, Y. Sun, L. Wang, C. Liu, Superhydrophobic TiO_2/polyvinylidene fluoride composite surface with reversible wettability switching and corrosion resistance, Chem. Eng. J. 290 (2016) 37–44.
[38] F. Su, K. Yao, Facile fabrication of superhydrophobic surface with excellent mechanical abrasion and corrosion resistance on copper substrate by a novel method, ACS Appl. Mater. Interfaces 6 (2014) 8762–8770.
[39] C. Chang, T. Huang, C. Peng, T. Yeh, H. Lu, W. Hung, C. Weng, T. Yang, J. Yeh, Novel anticorrosion coatings prepared from polyaniline/graphene composites, Carbon 50 (2012) 5044–5051.
[40] J. Li, R. Wu, Z. Jing, L. Yan, F. Zha, Z. Lei, One-step spray-coating process for the fabrication of colorful superhydrophobic coatings with excellent corrosion resistance, Langmuir 31 (2015) 10702–10707.
[41] R. Yuan, S. Wu, P. Yu, B. Wang, L. Mu, X. Zhang, Y. Zhu, B. Wang, H. Wang, J. Zhu, Superamphiphobic and electroactive nanocomposite toward self-cleaning, anti-wear, and anticorrosion coatings, ACS Appl. Mater. Interfaces 8 (2016) 12481–12493.
[42] T. Yeh, T. Huang, H. Huang, Y. Huang, Y. Cai, S. Lin, Y. Wei, J. Yeh, Electrochemical investigations on anticorrosive and electrochromic properties of electroactive polyuria, Polym. Chem. 3 (2012) 2209–2216.
[43] T. Huang, T. Yeh, H. Huang, W. Ji, Y. Chou, W. Hung, J. Yeh, M. Tsai, Electrochemical studies on aniline-pentamer-based electroactive polyimide coating: corrosion protection and electrochromic properties, Electrochim. Acta 56 (2011) 10151–10158.
[44] Z. Yu, H. Di, Y. Ma, L. Lv, Y. Pan, C. Zhang, Y. He, Fabrication of grapheme oxide–alumina hybrids to reinforce the anti-corrosion performance of composite epoxy coatings, Appl. Surf. Sci. 351 (2015) 986–996.